J. Condensed Matter Nucl. Sci. 36 (2022) 97–108

Research Article

Some Novel Analytical Techniques Applied to LENR Active Materials

Francis Tanzella*
Energy Research Center LLC, San Carlos, CA 94070, USA

Robert Godes and Robert George
Brillouin Energy Corporation, Berkeley, CA 94705 USA

Anis Rahman
Applied Research & Photonics, Inc., Harrisburg PA 17111 USA

Abstract

We explore the results from the analyses of several low energy nuclear reactions (LENR)-active tubes run by Brillouin Energy (BEC) using several different techniques. The most novel analytical techniques are terahertz (THz) imaging and THz spectroscopy. This imaging technique gives insight into the lattice spacing of crystalline and micro-crystalline metals and ceramics complimentary to that from X-ray diffraction (XRD) measurements. XRD of powder removed from this sample showed the normal lattice spacing for pure Ni powder. However, THz imaging showed lattice dilation in the Ni coating. We discuss the potential source of this dilation as well as its possible importance to LENR. We will also discuss the results of THz spectroscopy performed on materials from this and similar tubes This report discusses metallurgical and physical measurements, such as optical microscopy, density and porosity measurements, terahertz (THz) imaging and spectroscopy and scanning electron microscopy (SEM). We also cover chemical and elemental measurements such as energy dispersive X-ray (EDX) inductively coupled plasma-optical emission spectroscopy (ICP-OES), ICP-mass spectroscopy (ICP-MS) and He mass spectroscopy. With the latter method we present an intriguing result that shows tritium production in a unique Pd electrolysis experiment. EDX, ICP-OES, and ICP-MS can help the researcher understand the role of minor and major elemental impurities in these materials. If present, ICP-MS may also detect isotopic anomalies in these materials post experiment. The ultimate point of this exercise should be to help the LENR field reproduce the materials that are best suited for use in LENR experiments such as that presented as a worked example of designing and manufacturing a Pd rod from measurements like these.

Keywords: LENR, Metallurgy, Elemental analysis, Chemical analysis, Palladium

*Corresponding author: consulting@tanzella.name

© 2022 ICCF. All rights reserved. ISSN 2227-3123

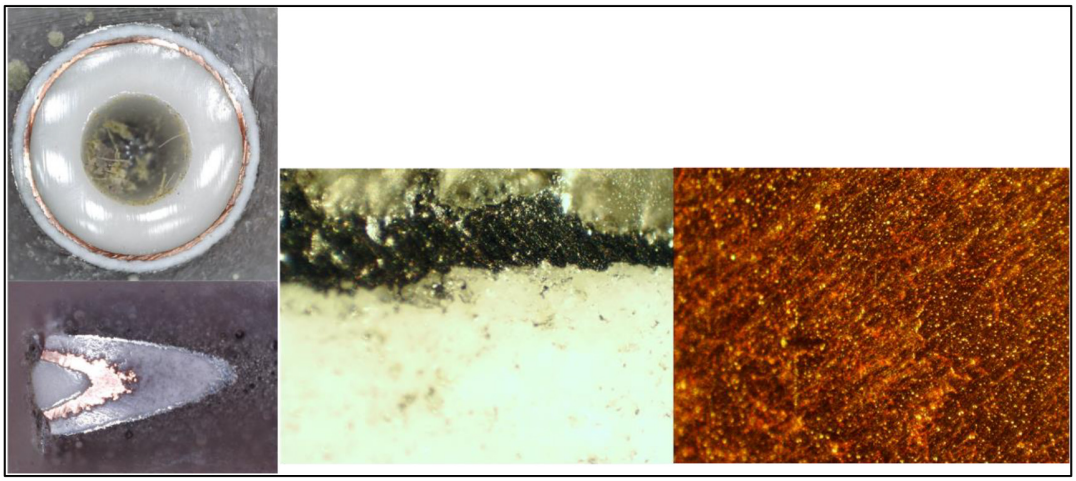

Figure 1. SEM micrographs of one of Brillouin's tubes.

1. Introduction

Since there has been a significant amount of discussion recently about finding the best material for low energy nuclear reactions (LENR), this paper discusses existing methods to determine the properties of the relevant materials used and to take the opportunity to introduce new techniques.

This report discusses metallurgical and physical measurements, such as optical microscopy, density and porosity measurements, terahertz (THz) imaging and spectroscopy and scanning electron microscopy (SEM) in the first half of the paper. The second half will cover chemical and elemental measurements such as energy dispersive X-ray (EDX) inductively coupled plasma-optical emission spectroscopy (ICP-OES), ICP-mass spectroscopy (ICP-MS) and He mass spectroscopy. Then we will end with a rather old worked example of designing and manufacturing a Pd rod from measurements like these.

2. Metallurgical and Physical Analyses

2.1. Optical Microscopy

The old-fashioned optical microscope can tell you quite a bit about your materials.

Figure 1 shows micrographs from two pieces of Brillouin Energy Corporation's three-layer coated tubes. These have been cut in a diamond saw, mounted in an epoxy casting resin, and sequentially polished from coarse grit sandpaper down to 1μm diamond paste on a buffing cloth. The upper left photo shows the cross-section of the tube after mounting and polishing. The white inner ring is the tubular ceramic substrate below the first coating of copper, followed by a plasma-sprayed ceramic coating and one of nickel. The distance from the inside the copper to outside of the nickel is approximately 400 μm. The lower left photo shows the tube mounted lengthwise with a metal shim holding it ∼4° from horizontal so the polishing exaggerates the depth radially. In the middle micrograph you can see the outer two layers of dielectric and Ni, and the epoxy, with the voids evident. The middle micrograph shows the voids in the ceramic coating. The micrograph on the right shows the Cu from the oblique cut sample exposing its less than 1 μm grains.

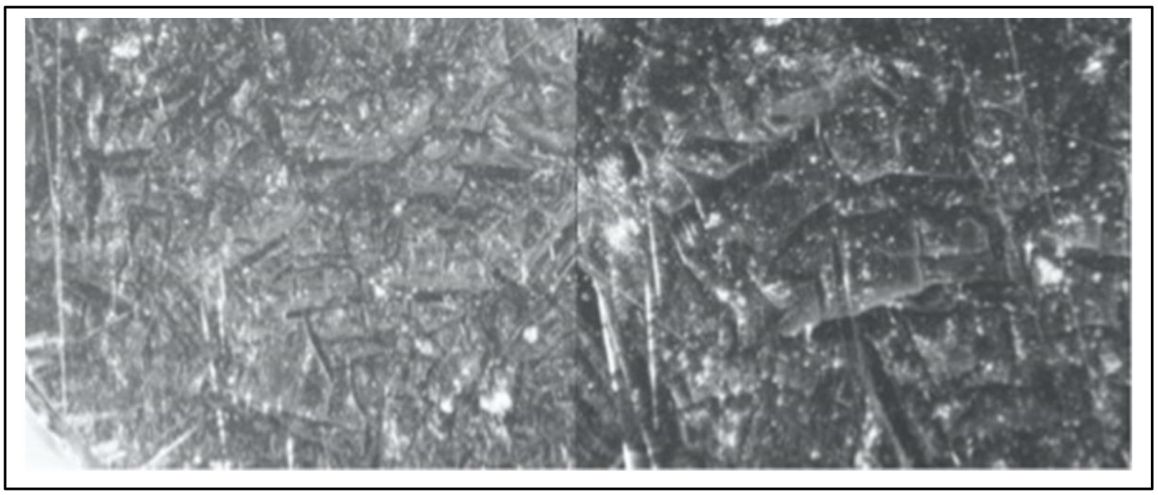

Figure 2. SEM micrographs of electrolysed Pd cathode.

In Figure 2 are two optical micrographs of a professionally cut, mounted and polished 3mm Pd cathode after a lithium deuteroxide electrolysis experiment from SRI International. The Pd grains and grain boundaries can be seen in both micrographs. The middle micrograph is about 130μm wide while the higher magnification one on the right is 52 μm wide. The color saturation and exposure has been adjusted the for better contrast in these two micrographs. After electrolysis the grains are about 5μm, probably oriented as received (drawn). Normally a researcher would make note of the grain size and orientation before use via non-destructive microscopy, for later comparison.

2.2. Density, Porosity and Stress/Strain Measurement

At SRI we regularly used instruments [1] regularly to characterize solids and powders. Although these instruments are normally used for catalyst and catalyst support materials, they can reveal important information about pure metals or metal/ceramic composites. Understanding the physical voids and internal surface area of cathodes and gas-exposed solids is important as recently noted. For pure materials, the measured density reveals the percent density of the actual material compared to that 100% dense. Knowing the non-molecular absorption or adsorption on the surface or in internal voids, allows one to better calculate how much of the hydrogen isotopes are in the interstitial sites. Various mechanical properties can be determined using instruments from Instron® [2].

2.3. X-Ray Diffraction

Another important physical measurement tool is X-ray diffraction. A powder or solid sample is held in a monochromatic X-ray beam while an X-ray detector is swung through an arc of 90° or more. The diffracted beam intensity is plotted against the angle in 2-theta. Generally, the resultant peaks are compared to a very large data base of known diffraction patterns. Impurities much below 1% are generally missed by this technique. The three major peaks shown in the diffractogram [3] in Figure 3 are from the face centered cubic (fcc) lattice of Ni. The minor peaks are from the alumina powder impurity, since this Ni was scraped from a Ni coating on top of alumina. The structure of unknown materials created during the LENR process may be determined using a process called the Reitveld refinement.

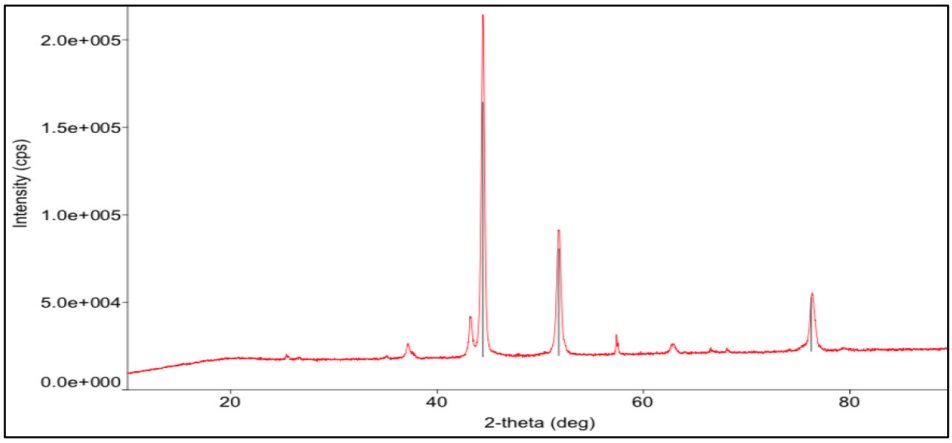

Figure 3. X-ray diffractogram of NI powder from one of Brillouin's tubes.

2.4. Terhertz Imaging and Spectroscopy

Recently, we have been practicing the THz imaging technology practiced Anis Rahman at Applied Research and Photonics. Rahman has published [4] calibrations that have shown that this technology yields the same measurement results seen via SEM and TEM on 14nm metal lines on Si wafers. By plotting the grayscale depth vs horizontal position across an image, the top being a black line and the bottom the white space peaks are seen. The FWHM of each peak, used to calculate the line width, averages to 15 $+/-$ 1 nm compared to the nominal 14nm lines. It is important to note that this technique overcomes the Abbe diffraction limit of traditional microscopic methods.

From a tube constructed similarly to that shown in earlier optical micrographs, the outer Ni coating was analyzed using THz imaging. The sample in its holder is shown in the left photograph. The image in the middle shows the lines seen from a 100nm x 100nm measurement [5]. Applying the analysis shown from the calibration, the FWHM measurement from the grayscale depth plot on the right gives a significantly greater lattice constant, as coated, than found by scraping some of the powder off and running X-ray powder diffraction. The plasma spraying process seems to have yielded Ni with a dilated lattice constant known as lattice expansion. This level of expansion would yield a unit cell volume approximately twice that of pure Ni. Representations of stationery and rotating cube images can also be produced by this technique.

Four similar samples were measured using these imaging and spectroscopic techniques [6]. THz spectroscopic measurements were collected from 0.1 to 32 THz. The THz laser spectrometer setup is shown in Figure 5. The absorbance spectrum from 0.1 to 10THz is also shown on the bottom right graph. Several peaks are noted in the range of those calculated for Ni phonon excitations. These are in a similar range to those reported by Dennis Letts [7] in his dual-laser beat-frequency experiment on Pd.

Figure 6 shows close ups of the same data from Figure 5 presented in wavenumber mode. The absorbance peaks are consistent with those reported in the literature for NiO. We predict that the Ni was oxidized after leaving the plasma spray gun and before cooling on the tube. Although the metal travels through a reducing atmosphere plasma at the spray gun, it traverses room air on its way to the target tube. There is still some work yet to be done in understanding these materials, before and after exposure to hydrogen in the reactors. Although these results agree with some published results, there are still unidentified peaks that should be able to tell us about the chemistry and physics of these coatings.

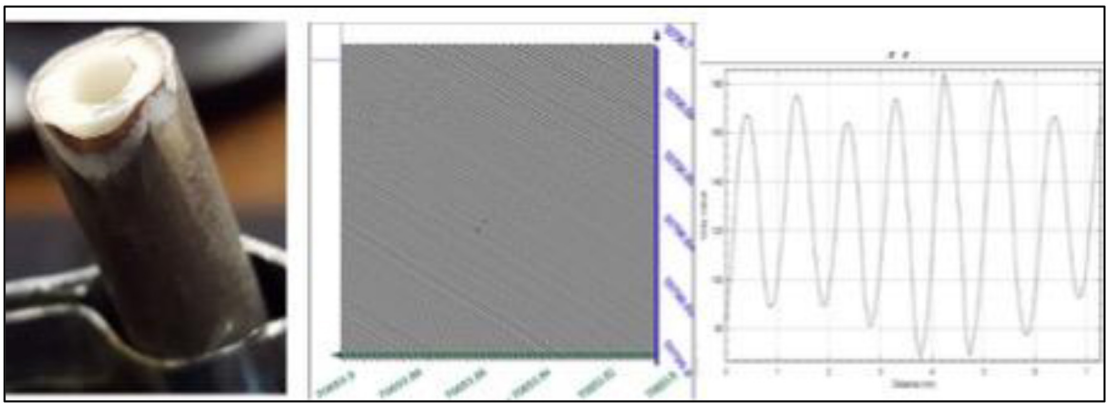

Figure 4. Sample and results from lattice-scale THz imaging measurement.

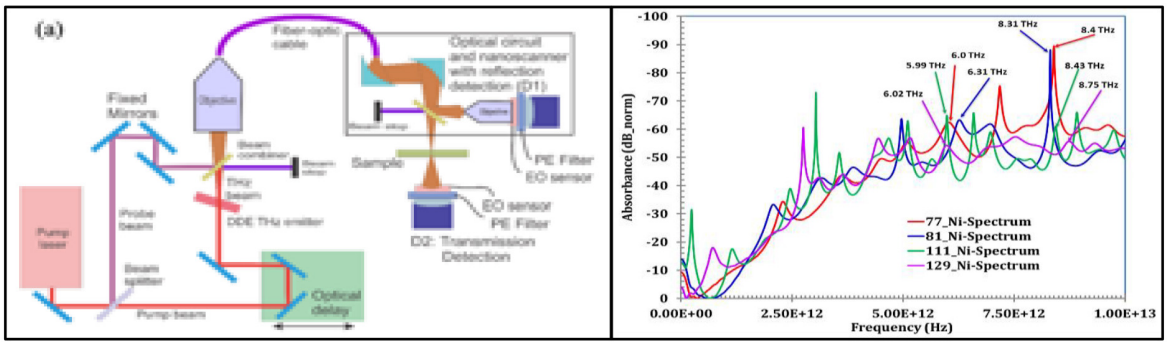

Figure 5. THz spectroscopic setup spectrum of Brillouin tube sample.

2.5. Scanning Electron Microscopy

Figure 7 displays three SEM micrographs taken by Alan Goldwater of MagicSound Labs, on Brillouin tubes similar to those shown earlier. The conducting materials show up as white and the insulators show up darker. The legend bar on the left two micrographs of the cross-section and oblique angle cut samples is 2mm. In this mounting the vertical direction is expanded by a factor of 10 in the oblique cut sample compared to that of the cross section. The legend bar on the lower right is 7μm, allowing for much finer measurements than in the optical photographs. Those green dots on the right micrograph are for EDX elemental composition measurements.

Figure 8 shows a micrograph of a Pd foil cathode of much higher magnification - 5,000x post experiment. This is from SRI's reproduction of Energetic Technologies SuperWave® electrolysis experiments [8]. Taken at the Naval Research Lab features of less than 1μm are visible. This sort of SEM can tell you quite a bit about a sample before and after exposure in a reactor.

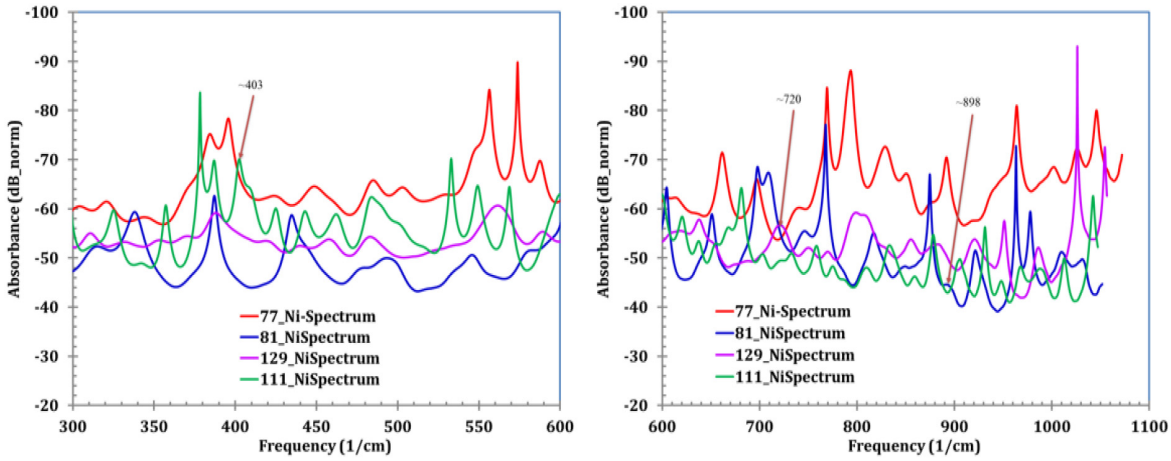

Figure 6. Wavenumber representation of THz spectrum form Brillouin tube sample.

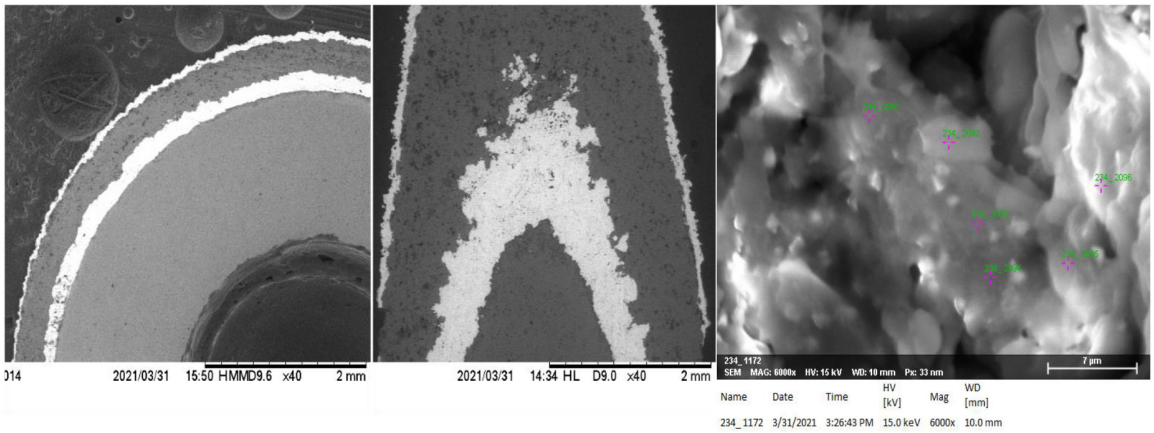

Figure 7. Scanning electron micrographs of pieces of a Brillouin coated tube.

3. Chemical and Elemental Analyses

3.1. Energy Dispersive X-Ray Analysis

Energy dispersive X-ray analysis uses the known X-ray energies of individual elements when exposed to an X-ray beam in the SEM's vacuum chamber. Figure 9 displays an EDX map of the same oblique cut sample shown in Figure 7 helps elucidate the sample's composition. These elemental maps taken by Alan Goldwater are a great visual aid in understanding what's going on in multi-layer coatings. The aluminum dominates both the sprayed and extruded Al_2O_3 map in the lower left map. However, the 5 images on the right show the Al in orange and the oxygen in red separately, which verifies the composition. The carbon map in yellow is from the epoxy mounting resin. The thin blue map is of the outer Ni coating. The inner Cu coating is shown in green.

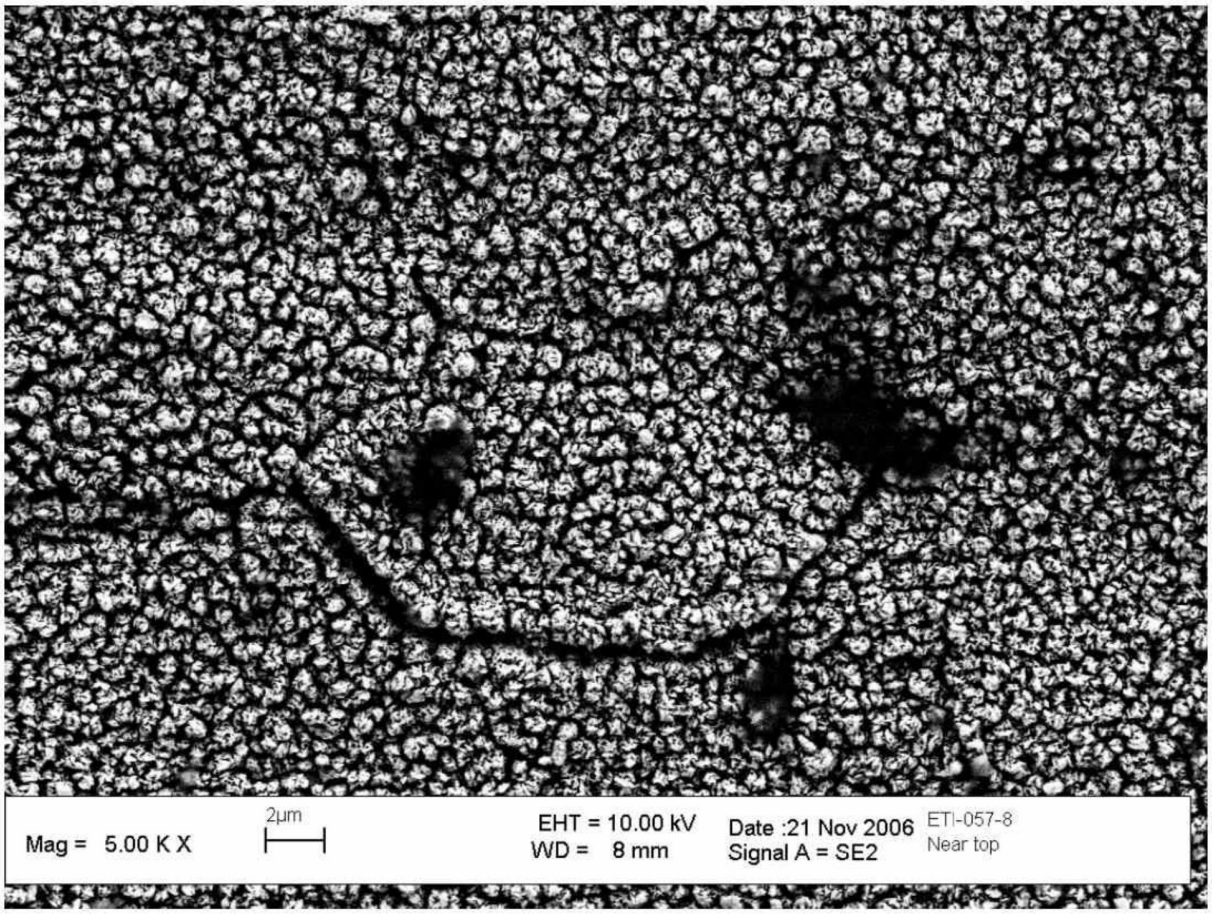

Figure 8. High magnification SEM image of electrolyzed Pd foil. (Courtesy of the Naval Research Laboratory).

Another way to view this multi-layer coating is from the cross-section sample. On the bottom left of Figure 10 is a thin section of a SEM image of this sample covering 682µm horizontal. The line designates where the EDX spectrometer has taken elemental measurements along the image, which is a novel way to view the elemental constituents across a multi-layered coating. In the graph in the upper left, which aligns with the SEM image, the red line designates the Ni composition, the blue line the aluminum in the dielectric, and the green line the Cu coating. The voids in the image line up with the reduced Al strength in the graph. There is obviously some sodium impurity (yellow line) in the Cu. The right image shows the elemental analyses of different points (green dots) in the SEM micrograph taken in the middle of the alumina coating. Although concentrations below 1 % are suspect, notice the 1.22 % sodium in the 234-2089 sample. It is interesting to note that the Al:O ratio is relatively constant. The carbon concentration is from machine background or from epoxy that moved into the voids during polishing.

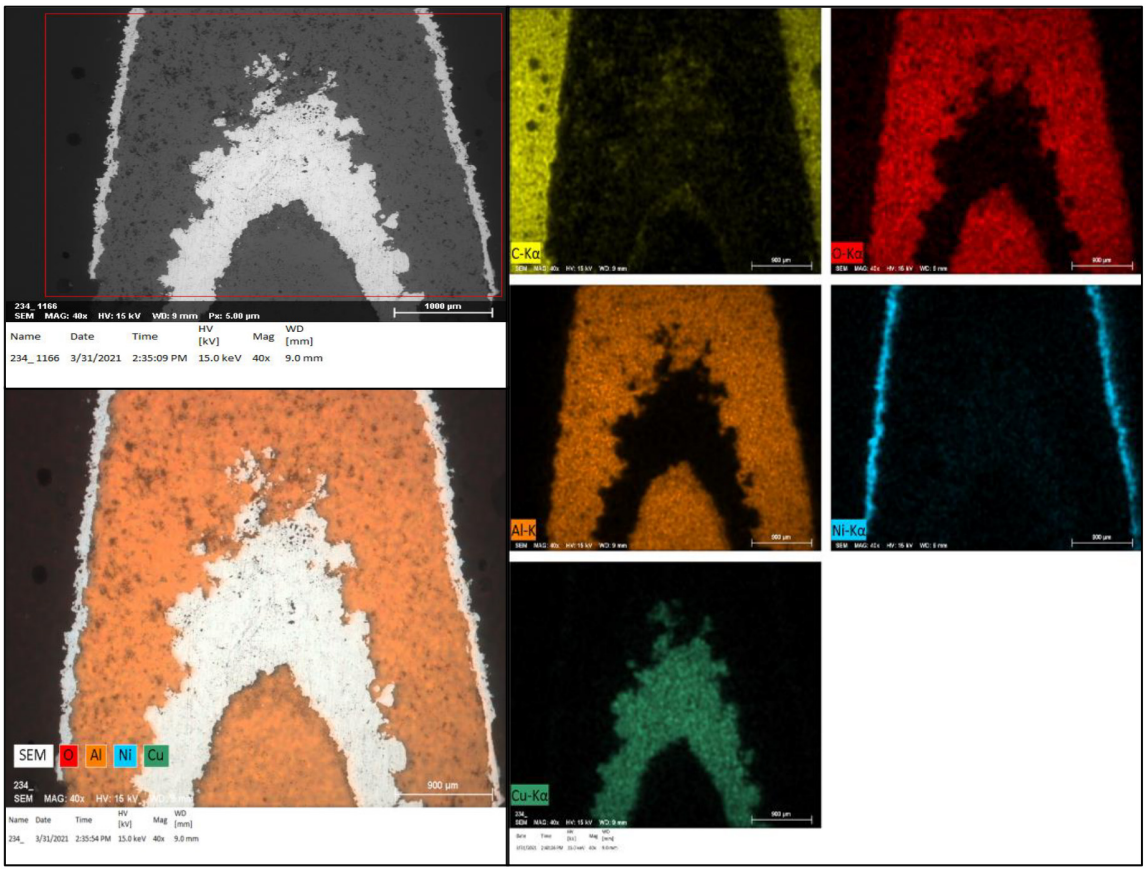

Figure 9. EDX elemental map of oblique-cut Brillouin tube sample.

3.2. X-Ray Fluorescence

A tool similar to EDX is X-ray fluorescence. It uses the same principle measuring the X-ray energies of materials exposed to incident X-rays to identify the elements present in solids, powders, and even liquids. As with XRD and EDX the results are usually compared to known library peaks, even though the X-ray peaks can be calculated from first principles. Impurities below the 1% level are generally not seen. The same powder scraped from the Brillouin coated rod and measured using XRD in Figure 3 was measured using an XRF instrument at SRI [9] and is shown in Figure 11. The middle-energy plot on this slide shows the nickel K-alpha and K-beta peaks, along with a minor amount of iron. Other elements called out in the plot are not detectable. The lower energy plot, not shown, also showed the aluminum from the alumina impurity. Unlike EDX, no vacuum is necessary for XRF measurements since it is performed in room air.

3.3. Inductively-Coupled Plasma Optical Emission Spectroscopy

ICP-optical emission spectroscopy is a destructive way to determine the major, minor, and impurity elements in a material. Because it obtains a spectrum from the emission of many elements, several elements can be analyzed for

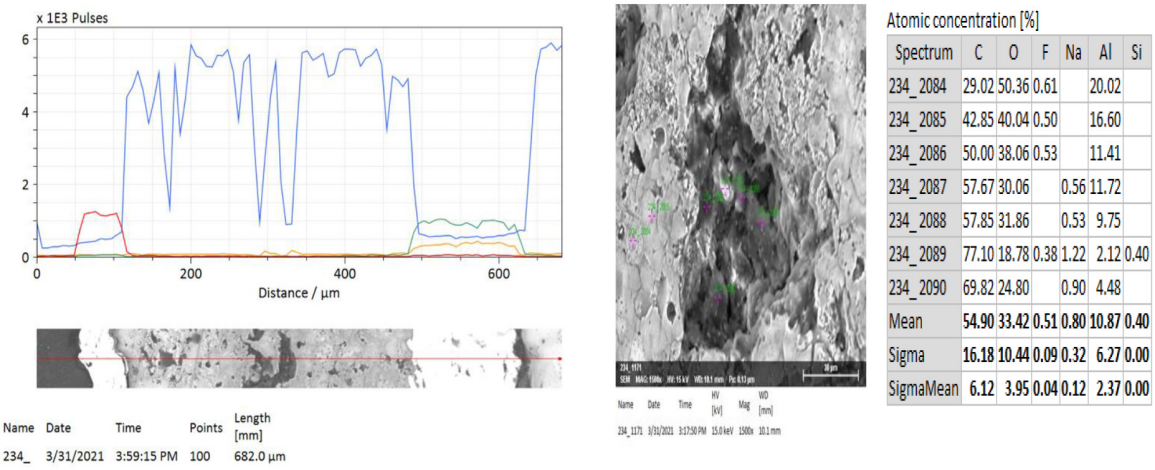

Atomic concentration [%]

Spectrum	C	O	F	Na	Al	Si
234_2084	29.02	50.36	0.61		20.02	
234_2085	42.85	40.04	0.50		16.60	
234_2086	50.00	38.06	0.53		11.41	
234_2087	57.67	30.06		0.56	11.72	
234_2088	57.85	31.86		0.53	9.75	
234_2089	77.10	18.78	0.38	1.22	2.12	0.40
234_2090	69.82	24.80		0.90	4.48	
Mean	**54.90**	**33.42**	**0.51**	**0.80**	**10.87**	**0.40**
Sigma	**16.18**	**10.44**	**0.09**	**0.32**	**6.27**	**0.00**
SigmaMean	**6.12**	**3.95**	**0.04**	**0.12**	**2.37**	**0.00**

Figure 10. EDX line-scan of a cross-section of a Brillouin tube sample.

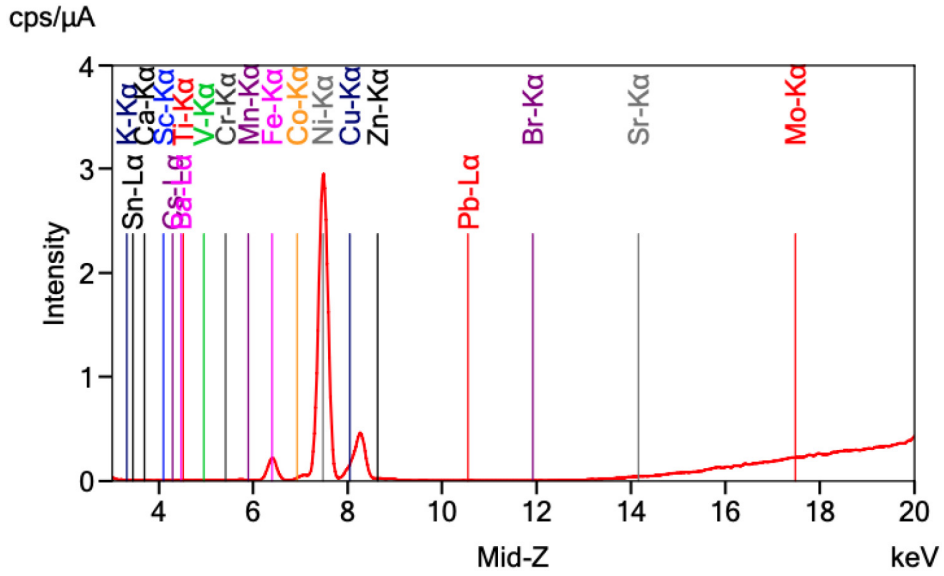

Figure 11. X-Ray fluorescence spectrum of nickel powder from Brillouin coated tube.

simultaneously, as opposed in the older atomic absorption method. Concentrations in the part per trillion level are common from ICP-OES analyses. The numbers in Table 1 have been normalized to the Ni major component. Results are usually reported as ppm or pptr. The analyses presented on Tables 1 and 2 are from Cerium Labs® in Austin Texas.

3.4. Inductively-Coupled Plasma Mass Spectroscopy

ICP-MS can tell you some of the same information that you get from ICP-OES, but may also tell you about isotopic changes in your material. Note the results in the bottom line of Table 2. The best way to assure reliable isotopic analysis is to use good isotopic standards. The example shown here has not been verified but is shown as a possible example analysis. In this case, the analyst felt that their mass resolution was not good enough to comfortably differentiate between Ni-64 and a possible Zn-64 impurity.

3.5. He Mass Spectroscopy

This measurement from SRI was first presented at ICCF11 [10]. He MS is another use of destructive metals analysis using mass spectrometry. This Arata double-structured cathode [11] consisted of a thick walled Pd bottle filled with Pd black and electrolyzed in D_2O for 3 months. Brian Clarke and Brian Oliver analyzed [12] the He-3 as an off-gas from the heated Pd black and Pd wall from this double-structured cathode, shown in Figure 12. Slicing up the wall as illustrated in the cartoon, they created a depth profile of He-3 from the inner wall to the outer wall of the cathodes from both experiments. The results from the D_2O experiment showed that the tritium produced in the inside diffused out achieving the expected concentration gradient as it decayed to He-3 along the way. A fair amount of tritium was also measured in the electrolyte from the D_2O experiment. No tritium or excess He-3 was measured in the H_2O experiment.

4. Palladium Rod Manufacture from these Type of Measurements

IMRA-Japan measured 21 different elements from a Pd rod that yielded impressive results. They also performed many of the other physical and chemical measurements listed in this paper. This was one of 42 samples subjected to this type of analyses. With the right capability, you can reproduce a desired material that my no longer be available. The details are not important but using these chemical analyses in addition to other materials analysis, IMRA Japan was

Table 1. ICP-OES analyses of samples from Brillouin's coated tubes.

Analyte Name	Al	Ba	Ca	Co	Cu	Na	Si	Sn	Zn
1N	1.545	1.933	0.307	1.005	0.752	N/D	0.381	0.362	4.127
2N	N/D	N/D	1631.5	N/D	115.507	11815.39	5212.185	483.268	N/D
3N	0.691	1.797	0.873	0.946	0.147	N/D	0.243	N/D	4.425
4N	0.113	0.017	N/D	0.009	0.121	0.0008	0.169	0.0007	0.0431

Table 2. ICP-MS isotopic results from a Brillouin Ni powder sample.

Analyte	Nominal Mass	Accurate Mass	Nominal Abundance	Ni Tube 75	Percent Diff
Ni	58	57.93535	68.27	65.74	3.77%
Ni	60	59.93079	26.10	25.17	3.62%
Ni	61	60.93106	1.13	1.21	6.70%
Ni	62	61.92835	3.59	3.89	8.06%
Ni	64	63.92797	0.91	3.99	125.65%

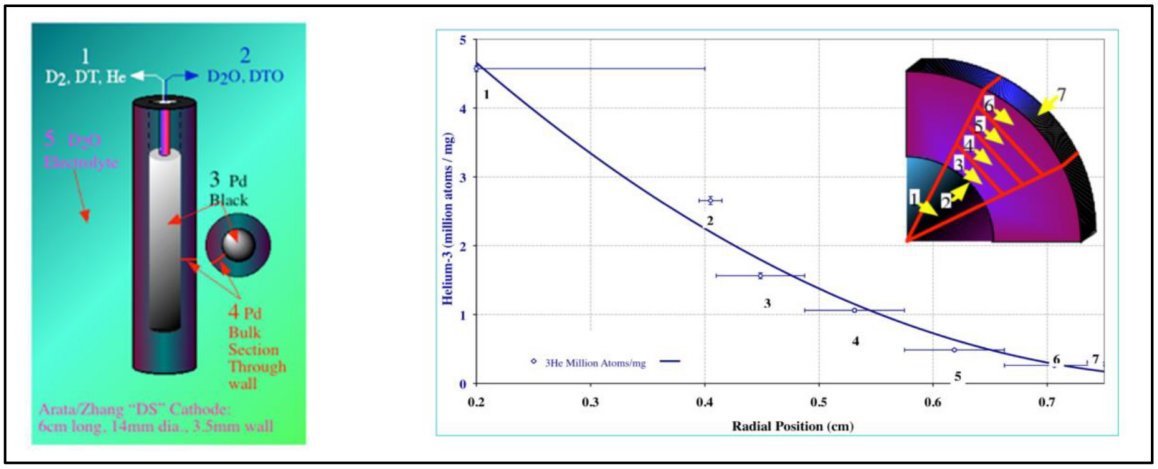

Figure 12. He-3 mass spec measurements from an electrolyzed double-structured cathode.

Figure 13. Palladium rod reproduced from extensive analyses of a good cathode.

able to reproduce one of these materials, shown in Figure 13. Many other Pd rods were produced for the NHE lab in Shin-Sapporo using these analyses.

5. Summary and Conclusions

The authors hope that the readers appreciate and the value of, and perform, some of these physical and chemical analysis techniques in documenting their better LENR materials.

Optical and electron microscopy and THz imaging can tell you about the metallurgy of metals and metal-ceramic composites. Density and surface area measurements can help you manufacture metals or powders that are LENR-active. EDX, ICP-OES, and ICP-MS can help understand the role of minor and major elemental impurities in these materials. If present, ICP-MS may also detect isotopic anomalies in these materials post experiment. In addition, you can produce pretty pictures to use in presentations to potential funders.

The ultimate point of this exercise may be to help the LENR field reproduce the materials that are best suited for use in LENR experiments such as that shown in Figure 13, or to create and verify the properties of a material of one's own design.

6. Acknowledgements

The authors would like to thank Alan Goldwater for the use of his images and results performed for Brillouin. We would like to acknowledge IMRA Japan for its analysis and Pd rod manufacture done for the NHE lab in Sapporo. The authors would also like to thank the Anthropocene Institute for its financial support.

References

[1] Micromeritics Instrument Corporation, https://www.micromeritics.com.
[2] Instron, https://www.instron.com/en/.
[3] Rigaku MiniFlex X-ray Diffraction Spectrometer, https://www.rigaku.com/products/xrd/miniflex
[4] A. Rahman and A. K. Rahman, IEEE Transactions on Semiconductor Manufacturing, **32**(1), 7-13, (2019)
[5] A. Rahman *et al*., Novel Research in Sciences, **2**(4), (2019), NRS.2019.2.000545. DOI.10.31031/NRS.2019.2.000545
[6] A. Rahman and D. Tomalia., Spectroscopy, **36**(4), 20-27 (2019).
[7] P. Hagelstein, D. Letts and D. Cravens, "Terahertz difference frequency response of PdD in two-laser experiments", Journal of Condensed Matter Nuclear Science, 3 (2010) 59.
[8] E. Castagna, E.; M. Sansovini, S. Lecci, A. Rufoloni, F. Sarto, V. Violante, D. Knies, K. S. Grabowski, G. K. Hubler, M. C. H. McKubre, F. L. Tanzella, "Metallurgical characterization of Pd electrodes employed in calorimetric experiments under electrochemical deuterium loading", Proceedings of 14th International Conference on Condensed Matter Nuclear Science, Washington, DC, (2008) 44.
[9] Rigaku NEX QC+ QuantEZ X-ray Fluorescence Spectrometer, https://www.rigaku.com/products/edxrf/quantez
[10] P. L. Hagelstein, M. C. H. McKubre, D. J. Nagel, T. A. Chubb, and R. Hekman. In New Physical Effects in Metal Deuterides, Eleventh International Conference on Condensed Matter Nuclear Science, Marseille, France, Marseille, France, 2004.
[11] Y. Arata and Y. C. Zhang, "Anomalous difference between reaction energies generated within D2O-cell and H2O-cell". Jpn. J. Appl. Phys. Part 2, 37 (1998) L1274.
[12] B. W. Clarke, B. M., Oliver; M. C. H. McKubre, F. L. Tanzella, and P. Tripodi, "Search for 3He and 4He in Arata-Style Palladium Cathodes II: Evidence for Tritium Production", Fusion Sci. & Technol. 40 (2001) 152.